

Athletic Intelligence Olympics challenge with Model-Based Reinforcement Learning

Dalla Libera, Alberto; Turcato, Niccolò; Giacomuzzo, Giulio; Carli, Ruggero; Romeres, Diego

TR2023-111 September 02, 2023

Abstract

In this report, we describe the solution we propose for the AI Olympics competition held at IJCAI 2023. Our solution is based on a recent Model-Based Reinforcement Learning algorithm named MC-PILCO. Besides briefly reviewing the algorithm, we discuss the most critical aspects of the MC-PILCO implementation in the environments at hand.

International Joint Conference on Artificial Intelligence 2023

© 2023 MERL. This work may not be copied or reproduced in whole or in part for any commercial purpose. Permission to copy in whole or in part without payment of fee is granted for nonprofit educational and research purposes provided that all such whole or partial copies include the following: a notice that such copying is by permission of Mitsubishi Electric Research Laboratories, Inc.; an acknowledgment of the authors and individual contributions to the work; and all applicable portions of the copyright notice. Copying, reproduction, or republishing for any other purpose shall require a license with payment of fee to Mitsubishi Electric Research Laboratories, Inc. All rights reserved.

Athletic Intelligence Olympics challenge with Model-Based Reinforcement Learning

Alberto Dalla Libera¹, Niccolo' Turcato¹, Giulio Giacomuzzo¹, Ruggero Carli¹ and Diego Romeres²

¹Department of Information Engineering, University of Padova, Italy.

²Mitsubishi Electric Research Laboratories, Cambridge, MA, USA.

alberto.dallalibera@unipd.it, turcatonic@dei.unipd.it, giulio.giacomuzzo@phd.unipd.it, carlirug@dei.unipd.it, romeres@merl.com

Abstract

In this report, we describe the solution we propose for the AI Olympics competition held at IJCAI 2023. Our solution is based on a recent Model-Based Reinforcement Learning algorithm named MC-PILCO. Besides briefly reviewing the algorithm, we discuss the most critical aspects of the MC-PILCO implementation in the environments at hand.

1 Introduction

In this short paper, we present the Reinforcement Learning (RL) [Sutton and Barto, 2018] approach we implemented to tackle the AI Olympics competition held at IJCAI 2023¹. Our algorithm, named Monte-Carlo Probabilistic Inference for Learning Control (MC-PILCO) [Amadio *et al.*, 2022], is a Model-Based (MB) RL algorithm that proved remarkably data-efficient in several low-dimensional benchmarks, such as a cart-pole, a ball & plate, and a Furuta pendulum, both in simulation and real setups. MC-PILCO exploits data collected by interacting with the system to derive a model of the system dynamics, and optimizes the policy by simulating the system, rather than optimizing the policy directly on the actual system. When considering physical systems, this kind of approach can be highly performing and more data-efficient than Model-Free (MF) solutions.

This paper is organized as follows: Section 2 introduces the goal and the settings of the competition. Section 3 presents the MC-PILCO algorithm. Section 4 reports the experiments that have been performed, finally Section 5 concludes the paper.

2 Goal of the competition

The challenge considers a 2 degrees of freedom (dof) underactuated pendulum [Wiebe *et al.*, 2022; Wiebe *et al.*, 2023] with two possible configurations. In the first configuration, also called Pendubot, the first joint, namely, the one attached to the base link is active, and the second is passive. Instead, in the second configuration, also named Acrobot, the first joint is passive and the second is actuated. For each configuration,

the competition's goal is to derive a controller that performs the swing-up and stabilization in the unstable equilibrium point of the systems. Both robots are underactuated, which makes the task particularly challenging from the control point of view. The systems are simulated at 500 Hz with a Runge-Kutta 4 integrator for an horizon of $T = 10$ s. Controllers are evaluated by a performance and a robustness score.

3 MC-PILCO for underactuated robotics

In the first part of this section we briefly review MC-PILCO, then, in the second part, we discuss its application to the considered problem.

3.1 MC-PILCO review

MC-PILCO is a MB policy gradient algorithm, in which GPs are used to estimate system dynamics and long-term state distributions are approximated with a particle-based method.

Consider a system with evolution described by the discrete-time unknown transition function $f : \mathbb{R}^{d_x} \times \mathbb{R}^{d_u} \rightarrow \mathbb{R}^{d_x}$:

$$\mathbf{x}_{t+1} = f(\mathbf{x}_t, \mathbf{u}_t) + \mathbf{w}_t, \quad (1)$$

where $\mathbf{x}_t \in \mathbb{R}^{d_x}$ and $\mathbf{u}_t \in \mathbb{R}^{d_u}$ are respectively the state and input of the system at step t , while \mathbf{w}_t is an independent white noise describing uncertainty influencing the system evolution. As usual in RL, a cost function $c(\mathbf{x}_t)$ encodes the task to be accomplished. A policy $\pi_\theta : \mathbf{x} \rightarrow \mathbf{u}$ that depends on the parameters θ selects the inputs applied to the system. The objective is to find policy parameters θ^* that minimize the cumulative expected cost, defined as follows,

$$J(\theta) = \sum_{t=0}^T \mathbb{E}[c(\mathbf{x}_t)], \quad (2)$$

where the initial state x_0 is sampled according to a given probability $p(\mathbf{x}_0)$.

MC-PILCO's consists of the succession of several attempts to solve the desired task, also called trials. Each trial consists of three main phases: (i) model learning, (ii) policy update, and (iii) policy execution. In the first trial, the GP model is derived from data collected with an exploration policy, for instance, a random exploration policy.

In the model learning step, previous experience is used to build or update a model of the system dynamics. The policy

¹https://ijcai-23.dfki-bremen.de/competitions/ai_olympics/

73 update step formulates an optimization problem whose objec-
 74 tive is to minimize the cost in eq. (2) w.r.t. the parameters of
 75 the policy θ . Finally, in the last step, the current optimized
 76 policy is applied to the system and the collected samples are
 77 stored to update the model in the next trials.

78 In the rest of this section, we give a brief overview of the
 79 main components of the algorithm and highlight their most
 80 relevant features.

81 Model Learning

82 MC-PILCO relies on GP Regression (GPR) to learn the sys-
 83 tem dynamics [Rasmussen, 2003]. In our previous work,
 84 [Amadio *et al.*, 2022], we presented a framework specifically
 85 designed for mechanical systems, named speed-integration
 86 model. Given a mechanical system with d degrees of free-
 87 dom, the state is defined as $\mathbf{x}_t = [\mathbf{q}_t^T, \dot{\mathbf{q}}_t^T]^T$ where $\mathbf{q}_t \in \mathbb{R}^d$
 88 and $\dot{\mathbf{q}}_t \in \mathbb{R}^d$ are, respectively, the generalized positions and
 89 velocities of the system at time t . Let T_s be the sampling time
 90 and assume that accelerations between successive time steps
 91 are constant. The following equations describe the one-step-
 92 ahead evolution of the i -th degree of freedom,

$$\dot{q}_{t+1}^{(i)} = \dot{q}_t^{(i)} + \Delta_t^{(i)} \quad (3a)$$

$$q_{t+1}^{(i)} = q_t^{(i)} + T_s \dot{q}_t^{(i)} + \frac{T_s}{2} \Delta_t^{(i)} \quad (3b)$$

93 where $\Delta_t^{(i)}$ is the change in velocity. MC-PILCO estimates
 94 the unknown function $\Delta_t^{(i)}$ from collected data by means
 95 of GPR. Each $\Delta_t^{(i)}$ is modeled as an independent GP, deno-
 96 ted f^i , with input vector $\tilde{\mathbf{x}}_t = [\mathbf{x}_t^T, \mathbf{u}_t^T]^T$, hereafter refer-
 97 red as GP input. Given an input-output training dataset
 98 $\mathcal{D}^{(i)} = \{\tilde{\mathbf{X}}, \mathbf{y}^{(i)}\}$, where the inputs are $\tilde{\mathbf{X}} = [\tilde{\mathbf{x}}_1^T, \dots, \tilde{\mathbf{x}}_n^T]^T$,
 99 and the outputs $\mathbf{y}^{(i)} = [y_1^{(i)}, \dots, y_n^{(i)}]^T$ are measurements of
 100 $\Delta_t^{(i)}$ at time instants $t = 0, \dots, T_{tr}$, GPR assumes the fol-
 101 lowing probabilistic model,

$$\mathbf{y}^{(i)} = f^i(\tilde{\mathbf{X}}) + \mathbf{e}, \quad (4)$$

102 where vector \mathbf{e} accounts for noise, defined a priori as zero
 103 mean independent Gaussian noise with variance σ_e^2 . The un-
 104 known function f^i is defined a priori as a GP with mean
 105 $m_{\Delta}^{(i)}$ and covariance defined by a kernel function $k(\tilde{\mathbf{x}}_{t_i}, \tilde{\mathbf{x}}_{t_j})$,
 106 namely, $f^i(\tilde{\mathbf{X}}) \sim N(m_{\Delta}^{(i)}, K_{\tilde{\mathbf{X}}\tilde{\mathbf{X}}})$, where the element of
 107 $K_{\tilde{\mathbf{X}}\tilde{\mathbf{X}}}$ at row r and column j is $E[\Delta_{t_r}^{(i)}, \Delta_{t_j}^{(i)}] = k(\tilde{\mathbf{x}}_{t_r}, \tilde{\mathbf{x}}_{t_j})$.
 108 The mean function $m_{\Delta}^{(i)}$ can be derived from prior knowledge
 109 of the system, or can be set as the null function if no informa-
 110 tion is available. Instead, as regards the kernel function, one
 111 typical choice to model continuous functions is the squared-
 112 exponential kernel:

$$k(\tilde{\mathbf{x}}_{t_i}, \tilde{\mathbf{x}}_{t_j}) := \lambda^2 e^{-\|\tilde{\mathbf{x}}_{t_i} - \tilde{\mathbf{x}}_{t_j}\|_{\Lambda}^2} \quad (5)$$

113 where λ and Λ are trainable hyperparameters tunable by max-
 114 imizing the marginal likelihood (ML) of the training samples
 115 [Rasmussen, 2003].

116 As explained in [Rasmussen, 2003], the posterior distribu-
 117 tions of each $\Delta_t^{(i)}$ given \mathcal{D}^i are Gaussian distributed, with

mean and variance expressed as follows:

$$\begin{aligned} \mathbb{E}[\hat{\Delta}_t^{(i)}] &= m_{\Delta}^{(i)}(\tilde{\mathbf{x}}_t) + K_{\tilde{\mathbf{x}}_t \tilde{\mathbf{X}}} \Gamma_i^{-1} (\mathbf{y}^{(i)} - m_{\Delta}^{(i)}(\tilde{\mathbf{X}})) \\ \text{var}[\hat{\Delta}_t^{(i)}] &= k_i(\tilde{\mathbf{x}}_t, \tilde{\mathbf{x}}_t) - K_{\tilde{\mathbf{x}}_t \tilde{\mathbf{X}}} \Gamma_i^{-1} K_{\tilde{\mathbf{X}} \tilde{\mathbf{x}}_t} \\ \Gamma_i &= K_{\tilde{\mathbf{X}} \tilde{\mathbf{X}}} + \sigma_i^2 I \end{aligned} \quad (6)$$

Then, also the posterior distribution of the one-step ahead
 transition model in (3) is Gaussian, namely,

$$p(\mathbf{x}_{t+1} | \mathbf{x}_t, \mathbf{u}_t, \mathcal{D}) \sim \mathcal{N}(\boldsymbol{\mu}_{t+1}, \Sigma_{t+1}) \quad (7)$$

with mean $\boldsymbol{\mu}_{t+1}$ and covariance Σ_{t+1} derived combining (3)
 and (6).

Policy Update

In the policy update phase, the policy is trained in order to
 minimize the expected cumulative cost in eq. (2) with the
 expectation computed w.r.t. the one-step ahead probabilistic
 model in eq. (7). This requires the computation of long-term
 distributions starting from the initial distribution $p(\mathbf{x}_0)$ and
 eq. (7), which is not possible in closed form. MC-PILCO
 resorts to Monte Carlo sampling [Caflich, 1998] to approx-
 imate the expectation in eq. (2). The Monte Carlo procedure
 starts by sampling from $p(\mathbf{x}_0)$ a batch of N particles and sim-
 ulates their evolution based on the one-step-ahead evolution
 in eq. (7) and the current policy. Then, the expectations in
 eq. (2) are approximated by the mean of the simulated parti-
 cles costs, namely,

$$\hat{J}(\theta) = \sum_{t=0}^T \left(\frac{1}{N} \sum_{n=1}^N c(\mathbf{x}_t^{(n)}) \right) \quad (8)$$

where $\mathbf{x}_t^{(n)}$ is the state of the n -th particle at time t .

The optimization problem is interpreted as a stochastic gra-
 dient descend problem (SGD) [Bottou, 2010], applying the
 reparameterization trick to differentiate stochastic operations
 [Kingma and Welling, 2013].

The authors of [Amadio *et al.*, 2022] proposed the use of
 dropout [Srivastava *et al.*, 2014] of the policy parameters θ to
 improve exploration and increase the ability to escape from
 local minima during policy optimization of MC-PILCO.

3.2 MC-PILCO for underactuated robotics

The task in object presents a number of practical issues when
 applying the algorithm. The first one is that the control fre-
 quency requested by the challenge is quite high for a MBRL
 approach. Indeed, high control frequencies require a high
 number of model evaluations which increases the computa-
 tional cost of the algorithm. Generally, this class of systems
 can be controlled at relatively low frequencies, for instance,
 [Amadio *et al.*, 2022] and [Amadio *et al.*, 2023] derived a
 MBRL controller for a Furuta Pendulum at 33 Hz. However,
 the physical properties of the simulated systems (no friction)
 make the system particularly sensitive to the system input.
 For these reasons, we selected a control frequency of 100 Hz.

The second issue is that controllers are evaluated by a per-
 formance and robustness score. In the robustness test, the
 characteristics of the system and data acquisition vary. This

162 is an issue for data-driven solutions like MC-PILCO since re-
 163 training of the controller is not allowed. For this reason, we
 164 decided to focus only on the performance score, even if in
 165 our previous work we showed that MC-PILCO can be robust
 166 to noise and filtering by including these effects in the simulation.
 167

168 Since the nominal model of the system is available to de-
 169 velop the controller, we use the forward dynamics function of
 170 the plant as the prior mean function of the change in velocity
 171 for each joint. The available model is

$$B\mathbf{u}_t = M(\mathbf{q}_t)\ddot{\mathbf{q}}_t + n(\mathbf{q}_t, \dot{\mathbf{q}}_t), \quad (9)$$

172 where $M(\mathbf{q}_t)$ is the mass matrix, $n(\mathbf{q}_t, \dot{\mathbf{q}}_t)$ contains the
 173 Coriolis, gravitational and damping terms, and B is the ac-
 174 tuation matrix, which is $B = \text{diag}([1, 0])$ for the Pendubot
 175 and $B = \text{diag}([0, 1])$ for the Acrobot. We define then

$$m_\Delta(\tilde{\mathbf{x}}_t) = \begin{bmatrix} m_\Delta^{(1)} \\ m_\Delta^{(2)} \end{bmatrix} := T_s \cdot M^{-1}(\mathbf{q}_t)(B\mathbf{u}_t - n(\mathbf{q}_t, \dot{\mathbf{q}}_t)) \quad (10)$$

176 as the mean function in eq. (6). It is important to point out that
 177 eq. (10) is nearly perfect to approximate the system when T_s
 178 is sufficiently small, but it becomes unreliable as T_s grows. In
 179 particular, with $T_s = 0.01$ s the predictions of eq. (10) are not
 180 good enough to describe the behavior at the unstable equilib-
 181 rium. The inaccuracies of the prior mean are compensated by
 182 the GP models. To cope with the large computational burden
 183 due to the high number of collected samples, we implemented
 184 the GP approximation Subset of Regressors, see [Quiñonero-
 185 Candela and Rasmussen, 2005] for a detailed description.

186 An important aspect of policy optimization is the particles
 187 initialization, in this case, it is guaranteed that the system will
 188 always start at $\mathbf{x}_0 = \bar{0}$, therefore the initial distribution can
 189 be set to $p(\mathbf{x}_0) \sim \mathcal{N}(\bar{0}, \epsilon I)$ with ϵ in the order of 10^{-4} .

The cost function must evaluate the policy performance
 w.r.t. the task requirements, in this case, we want the system
 to reach the position $\mathbf{q}_G = [\pi, 0]^T$ and stay there indefinitely.
 A cost generally used in this kind of system is the saturated
 distance from the target state:

$$c_{st}(\mathbf{x}_t) = 1 - e^{-\|\mathbf{q}_t - \mathbf{q}_G\|_{\Sigma_c}^2} \quad \Sigma_c = \text{diag}\left(\frac{1}{\ell_c}, \frac{1}{\ell_c}\right), \quad (11)$$

190 with $\ell_c = 3$. Notice that this cost does not depend on the
 191 velocity of the system, just on the distance from the goal state,
 192 but it does encourage the policy to reach the goal state with
 193 zero velocity.

194 The policy function that is used to learn a control strategy
 195 is the general purpose policy from [Amadio *et al.*, 2022]:

$$\pi_\theta(\mathbf{x}_t) = u_M \tanh\left(\sum_{i=1}^{N_b} \frac{w_i}{u_M} e^{-\|\mathbf{a}_i - \phi(\mathbf{x}_t)\|_{\Sigma_\pi}^2}\right) \quad (12)$$

$$\phi(\mathbf{x}_t) = [\dot{\mathbf{q}}_t^T, \cos(\mathbf{q}_t^T), \sin(\mathbf{q}_t^T)]^T$$

196 with hyperparameters $\theta = \{\mathbf{w}, A, \Sigma_\pi\}$, where $\mathbf{w} =$
 197 $[w_1, \dots, w_{N_b}]^T$ and $A = \{\mathbf{a}_1, \dots, \mathbf{a}_{N_b}\}$ are, respectively,
 198 weights and centers of the N_b Gaussians basis functions,
 199 whose shapes are determined by Σ_π . For both robots, the
 200 dimensions of the elements of the policy are: $\Sigma_\pi \in \mathbb{R}^{6 \times 6}$,

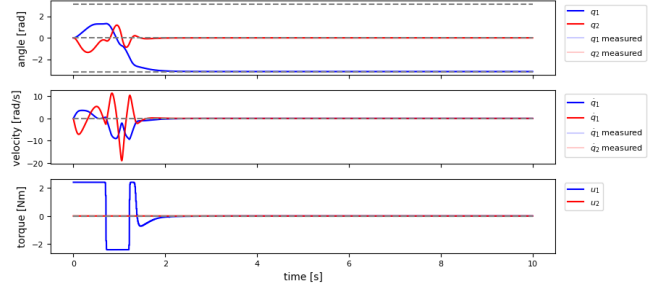


Figure 1: Simulation of the Pendubot system (500 Hz), under control of the policy trained with MC-PILCO.

Controller	Perf. score	Rob. score	Avg. score
TVLQR	0.827	0.95	0.8885
MC-PILCO	0.891	0.871	0.881
iLQR MPC stab.	0.845	0.86	0.8525
iLQR Riccati	0.847	0.592	0.7195
iLQR MPC	0.861	0.2	0.5305
Energy PFL	0.594	0.117	0.3555

Table 1: Pendubot scores comparison.

201 $\mathbf{a}_i \in \mathbb{R}^6$, $w_i \in \mathbb{R}$ for $i = 1, \dots, N_b$, since the policy outputs
 202 a single scalar. In the experiments, the parameters are initial-
 203 ized as follows. The basis weights are sampled uniformly in
 204 $[-u_M, u_M]$, the centers are sampled uniformly in the image
 205 of ϕ with $\dot{\mathbf{q}}_t \in [-2\pi, 2\pi]$ rad/s. The matrix Σ_π is initialized
 206 to the identity. Given the ideal conditions considered in this
 207 simulation, for the purpose of the challenge we switched to an
 208 LQR controller after swing-up. Under ideal circumstances,
 209 the LQR controller has the capability to stabilize the system
 210 at an unstable equilibrium by exerting zero final torque.

4 Experiments 211

212 In this section, we briefly discuss how the algorithm was ap-
 213 plied to both systems and show the main results. We also re-
 214 port the optimization parameters used for both systems, all
 215 the parameters not specified are set to the values reported
 216 in [Amadio *et al.*, 2022]. All the code was implemented in
 217 Python with the PyTorch [Paszke *et al.*, 2017] library.

218 For both robots, we use the model described in Section 3.1,
 219 with mean function from eq. (10) and kernel function from
 220 eq. (5). The max torque u_M was set to conservative values, to
 221 optimize the score of the controller. The policy optimization
 222 horizon was set much lower than the horizon required for the
 223 competition, this allows to reduce the computational burden
 224 of the algorithm, moreover, it pushes the optimization to find
 225 policies that can execute a fast swing-up. We exploit dropout
 226 in the policy optimization as a regularization strategy, to yield
 227 better policies.

4.1 Pendubot 228

229 The policy for the Pendubot swing-up was optimized for a
 230 horizon of $T = 3.0$ s, with u_M set to 40% of the torque
 231

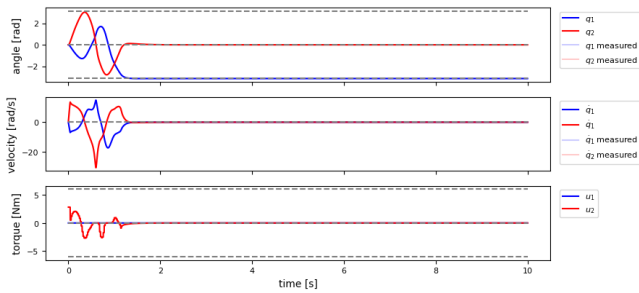


Figure 2: Simulation of the Acrobot system (500 Hz), under control of the policy trained with MC-PILCO.

5 Conclusions

In both systems, our MBRL approach reaches a performance score higher than other tested approaches, while remaining competitive w.r.t. the robustness score.

References

- [Amadio *et al.*, 2022] Fabio Amadio, Alberto Dalla Libera, Riccardo Antonello, Daniel Nikovski, Ruggero Carli, and Diego Romeres. Model-based policy search using monte carlo gradient estimation with real systems application. *IEEE Transactions on Robotics*, 38(6):3879–3898, 2022.
- [Amadio *et al.*, 2023] Fabio Amadio, Alberto Dalla Libera, Daniel Nikovski, Ruggero Carli, and Diego Romeres. Learning control from raw position measurements, 2023.
- [Bottou, 2010] Léon Bottou. Large-scale machine learning with stochastic gradient descent. In *Proc of COMPSTAT’2010*, pages 177–186. Springer, 2010.
- [Caffisch, 1998] Russel E Caffisch. Monte carlo and quasi-monte carlo methods. *Acta numerica*, 7:1–49, 1998.
- [Kingma and Welling, 2013] Diederik P Kingma and Max Welling. Auto-encoding variational bayes. *arXiv preprint arXiv:1312.6114*, 2013.
- [Paszke *et al.*, 2017] Adam Paszke, Sam Gross, Soumith Chintala, Gregory Chanan, Edward Yang, Zachary DeVito, Zeming Lin, Alban Desmaison, Luca Antiga, and Adam Lerer. Automatic differentiation in pytorch. 2017.
- [Quiñonero-Candela and Rasmussen, 2005] Joaquin Quiñonero-Candela and Carl Edward Rasmussen. A unifying view of sparse approximate gaussian process regression. *Journal of Machine Learning Research*, 6(65):1939–1959, 2005.
- [Rasmussen, 2003] Carl Edward Rasmussen. Gaussian processes in machine learning. In *Summer school on machine learning*, pages 63–71. Springer, 2003.
- [Srivastava *et al.*, 2014] Nitish Srivastava, Geoffrey Hinton, Alex Krizhevsky, Ilya Sutskever, and Ruslan Salakhutdinov. Dropout: a simple way to prevent neural networks from overfitting. *JMLR*, 15(1):1929–1958, 2014.
- [Sutton and Barto, 2018] Richard S Sutton and Andrew G Barto. *Reinforcement learning: An introduction*. MIT press, 2018.
- [Wiebe *et al.*, 2022] Felix Wiebe, Shubham Vyas, Lasse Jenning Maywald, Shivesh Kumar, and Frank Kirchner. Realaigym: Education and research platform for studying athletic intelligence. In *RSS Online Proceedings, Mind the Gap: Opportunities and Challenges in the Transition Between Research and Industry*, New York, 2022.
- [Wiebe *et al.*, 2023] Felix Wiebe, Shivesh Kumar, Lasse Shala, Shubham Vyas, Mahdi Javadi, and Frank Kirchner. An open source dual purpose acrobot and pendubot platform for benchmarking control algorithms for underactuated robotics. *IEEE Robotics and Automation Magazine*, 2023. under review.

limit of the actuator. The sampling time for model and policy learning is 0.01 s, thus the control rate is 100 Hz. The condition for switching to the LQR stabilization is $q_1 > 3.1$ rad. The Controller’s strategy is depicted in fig. 1, in fig. 3 (left) we report the robustness bar charts. This controller has a performance score of 0.891 and a robustness score of 0.852. In table 1 we compare our controller’s score with other tested control strategies.

4.2 Acrobot

The policy for the Pendubot swing-up was optimized for a horizon of $T = 3.0$ s, with u_M set to 50% of the torque limit of the actuator. The sampling time for model and policy learning is 0.02 s, thus the control rate is 50 Hz. The condition for switching to the LQR stabilization is $q_1 > 2.8$ rad. The Controller’s strategy is depicted in fig. 2, in fig. 3 (right) we report the robustness bar charts. This controller has a performance score of 0.869 and a robustness score of 0.73. In table 2 we compare our controller’s score with other tested control strategies.

Controller	Perf. score	Rob. score	Avg. score
TVLQR	0.783	0.861	0.822
MC-PILCO	0.869	0.634	0.7515
iLQR MPC stab.	0.806	0.685	0.7459
Energy PFL	0.728	0.503	0.6155
iLQR Riccati	0.831	0.298	0.5645
iLQR MPC	0.796	0.089	0.4425

Table 2: Acrobot scores comparison.

251

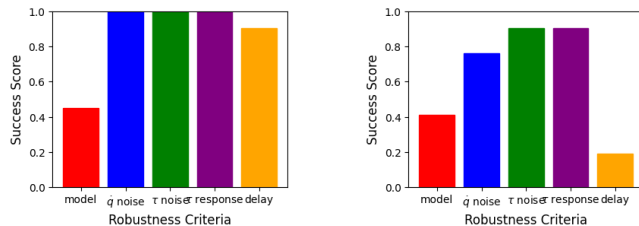


Figure 3: Pendubot (left) and Acrobot (right) robustness bar charts.

252
253
254
255
256
257
258
259
260
261
262
263
264
265
266
267
268
269
270
271
272
273
274
275
276
277
278
279
280
281
282
283
284
285
286
287
288
289
290
291
292
293
294
295
296
297
298
299
300
301
302
303